Steel and Composite Structures, Vol. 1, No. 4 (2001) 411-426
DOI: http://dx.doi.org/10.12989/scs.2001.1.4.411

Failure analysis of prestressing steel wires

J. Toribio†

Department of Materials Engineering, University of Salamanca, E.P.S., Campus Viriato, Avda. Requejo 33, 49022 Zamora, Spain

A. Valiente†

Department of Materials Science, Polytechnic University of Madrid, ETSI Caminos, Ciudad Universitaria, 28040 Madrid, Spain

Abstract. This paper treats the failure analysis of prestressing steel wires with different kinds of localised damage in the form of a surface defect (crack or notch) or as a mechanical action (transverse loads). From the microscopical point of view, the micromechanisms of fracture are *shear dimples* (associated with localised plasticity) in the case of the transverse loads and *cleavage-like* (related to a weakest-link fracture micromechanism) in the case of cracked wires. In the notched geometries the microscopic modes of fracture range from the ductile *micro-void coalescence* to the brittle cleavage, depending on the stress triaxiality in the vicinity of the notch tip. From the macroscopical point of view, fracture criteria are proposed as design criteria in damage tolerance analyses. The transverse load situation is solved by using an upper bound theorem of limit analysis in plasticity. The case of the cracked wire may be treated using fracture criteria in the framework of linear elastic fracture mechanics on the basis of a previous finite element computation of the stress intensity factor in the cracked cylinder. Notched geometries require the use of elastic-plastic fracture mechanics and numerical analysis of the stress-strain state at the failure situation. A fracture criterion is formulated on the basis of the critical value of the effective or equivalent stress in the Von Mises sense.

Key words: prestressing steel wires; fracture criteria; damage tolerance; structural integrity; engineering safe design.

1. Introduction

In recent years, damage tolerance approaches are progressively being introduced in structural engineering by means of improvement of recommendations included in the Standards, e.g., Eurocode 3 (CEN 1992) which are more or less based on fracture mechanics assumptions. The damage undergone by the structural material may consist of loss of physical continuity (*cracks*), loss of material itself (*notches*) or formation of weak zones by local degradation (*damaged areas*). The latter lead to cracks or notches when the material is so degraded that it breaks completely or loses its mechanical resistance, so that it can be modelled as a crack or notch, which are the two basic geometries in damage tolerance analyses.

In the case of prestressed concrete structures, different types of damage are frequently met because of

†Professor

constructional details such as anchorages or due to cyclic loading conditions (fatigue) or harsh environments (stress corrosion cracking), as described by Elices (1985). The types of localised damage may be classified according to the degree of triaxiality from the case of a smooth bar under transverse loads (minimum triaxiality level, maximum deviatoric stress) to the case of the cracked wire under tension loading (maximum triaxiality level, maximum hydrostatic stress). The notched bar in tension represents an intermediate stress state whose triaxiality level is a function of the geometry of the notch. While in the case of the smooth wire under transverse load the triaxiality of the stress state is created by the loading conditions, in the notched and cracked bars the stress triaxiality is created by the geometry itself.

The final aim of this paper is the review of fracture criteria useful as design criteria in structural engineering, covering different practical situations with different degree of triaxiality: the smooth wire under transverse load, and both the notched bar and the cracked wire under tension loading. This is a very important topic in damage tolerance approaches because, as explained in previous paragraphs, it may be assumed that many different kinds of material degradation zones behave as cracks or notches.

2. Smooth wires under transverse load

This problem was addressed in a previous paper (Valiente *et al.* 1988) whose purpose was to find a failure criterion for a prestressing steel wire under the simultaneous action of both an axial tensile load and a transverse local compression load which increases the deviatoric stress tensor and enhances failure of the wire.

Transverse compressions appear in the vicinity of anchorages, in supports of the tendon sheaths and in the places where tendons change their direction. It is known that this kind of loading reduces the strength of the reinforcements and thus two problems arise for structural engineers: the evaluation of the strength losses and the selection of appropriate steels.

A rigorous form to deal with the problem is a fracture mechanics approach. The knowledge of the fracture criterion for a wire under the simultaneous action of a longitudinal (axial) tension and a transverse local compression could contribute to the solution of practical engineering questions such as:

(a) predicting the strength losses due to transverse loads acting on the tensile member simultaneously to the main load,

(b) providing theoretical bases for characterising the transverse load resistance of prestressing steels by means of technological tests,

(c) supporting any quantitative definition of transverse load tolerance in the framework of fracture mechanics and damage tolerance approaches.

Experimental work covered the design and construction of a testing system able to apply simultaneously a longitudinal (axial) tensile load and a local transverse compression, in a similar manner to actual loading in service. To this end, a special experimental device was designed as shown in Fig. 1. The tensile load was applied in conventional manner by means of a universal testing machine with mechanical grips (main loading axis in vertical direction in Fig. 1). At the same time, a transverse compressive load was applied in a direction perpendicular to the main loading axis (this perpendicular direction being horizontal in Fig. 1) by means of a rigid frame (small if compared with the main frame which defines the testing area of the universal testing machine) and a small hydraulic cylinder which

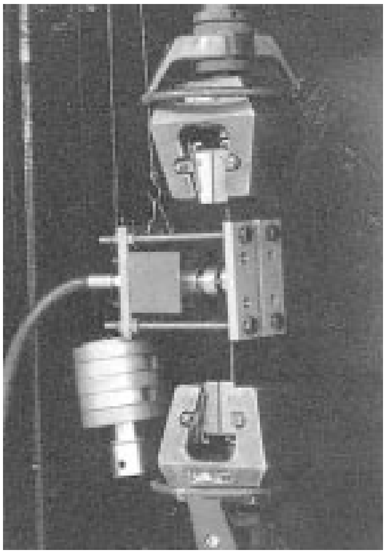

Fig. 1 Experimental device used in the tensile tests under transverse load. Tensile load: main loading axis in vertical direction (applied by the grips of the testing machine). Transverse compressive load: applied in horizontal direction by means of a small hydraulic cylinder

allows the choice of the transverse load by using oil pressure. This special purpose system allows the application of transverse loads ranging from 0 to 23 kN with a maximum error of ±0.12 kN.

Using this testing system, two structural materials were used in the experimental programme. Both were commercial prestressing steels in the form of high strength cold drawn wires whose diameters and mechanical properties are given in Table 1. Experimental results showed that both steels exhibited a marked loss of strength as the transverse load was increased, i.e., there is an inverse relationship between the critical axial load at the failure instant and the magnitude of the local transverse compression. In addition, ductility parameters such as the elongation at fracture also decreases as a consequence of the lateral compressive force.

From the microscopical point of view, the fracture micromechanisms are *shear dimples* associated with localised plasticity. Certain shear lips may be observed in the macroscopic fracture surfaces, which indicates that fracture initiates and propagates by shear following glide planes, i.e., a purely ductile failure micromechanism could be operative in this case. This fact allows the formulation of a macroscopic failure criterion according to the experimental results and the physical characteristics of the fracture surfaces in the tests.

A failure model was proposed, on assuming a planar fracture surface oriented an angle of 45^{o} in relation to the wire axis, because this angle agrees fairly well with that experimentally measured on the broken specimens. As the mechanism of failure is by shear (typically ductile), the theoretical approach to the problem can be the application of the classical theory of plasticity to the failure situation. Fig. 2 shows the failure mechanism considered for the limit analysis, consisting of the appearance of a shear band of width δ and oriented 45^{o} from the wire axis, as a consequence of the compressive transverse load of magnitude Q.

On the basis of the upper bound theorem of limit analysis in plasticity (Johnson and Mellor 1986) and

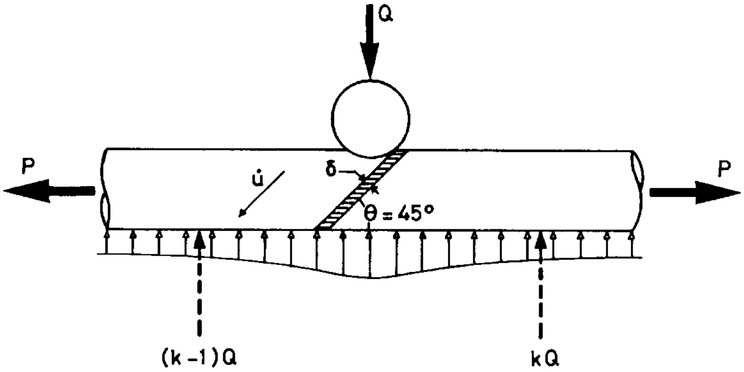

Fig. 2 Mechanism of failure in a wire subjected to the simultaneous action of an axial tensile load P and a transverse compressive load Q

applying the Tresca yield criterion to the mechanism proposed in Fig. 2, it is possible to bound a failure locus and thus to obtain the maximum shear failure condition. The external rate of work of the applied forces is:

$$\dot{W}_e = P\dot{u}\cos\theta + kQ\dot{u}\sin\theta \tag{1}$$

where all the symbols are given in Fig. 2. It was assumed that the distribution of reactions in the rigid plate opposite to the hydraulic cylinder (cf. Fig. 1) is equivalent to two reaction forces (k-1) Q and k Q.

On the other hand, the rate of internal energy dissipation has to be computed in the band of width δ as:

$$\dot{W}_i = \int_V \tau_Y\dot{\gamma}dV = \tau_Y\frac{\dot{u}}{\delta}\int_V dV \tag{2}$$

where τ_Y is the critical shear stress at yielding, γ the shear strain and V the volume of the band. it should be noted that, according to the model proposed in Fig. 2, the rate of shear strain is constant within the band. As the volume of this latter is $\Omega\delta/\sin\theta$ (where Ω is the transverse cross section of the wire), the rate of internal energy dissipation may be written as:

$$\dot{W}_i = \tau_Y\dot{u}\frac{\Omega}{\sin\theta} \tag{3}$$

Applying the upper bound theorem of plasticity (Johnson and Mellor 1986), the rate of work of the applied forces given in Eq. (1) must be lower than the rate of internal energy dissipation given in Eq. (3):

$$P\cos\theta + k\mathrm{Q}\sin\theta \leq \tau_Y\frac{\Omega}{\sin\theta} \tag{4}$$

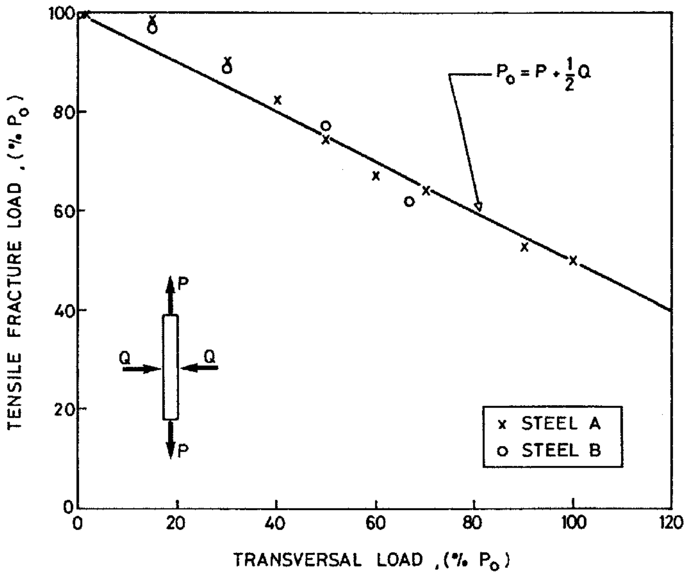

Fig. 3 Experimental results of the fracture tests under transverse load and failure locus

Table 1 Mechanical properties of the steels used in the experiments under transverse load

Steel	Diameter of the wire (mm)	Young's Modulus E (GPa)	Yield Strength σ_Y (MPa)	U.T.S. σ_R (MPa)	Elongation at UTS (%)
A	3.5	203	1550	1640	3
B	5	210	1610	1810	6.5

Finally, considering that $2\tau_Y\Omega$ is the failure load P_0 of the wire under pure tension (according to the Tresca yield criterion), and taking $\theta = 45°$ (see Fig. 2), the following expression is obtained:

$$P + k\,Q \leq P_0 \tag{5}$$

The limit case is the failure locus $P + k\,Q = P_0$, where P is the axial tensile load, Q is the lateral compression, P_0 is the maximum load in tension and k a dimensionless coefficient (a fitting parameter). Fig. 3 plots the experimental results of steels A and B (cf. Table 1), where a value $k = 0.5$ seems to be adequate for the prestressing steels tested in this research.

Therefore, a failure criterion for prestressing steel wires under the simultaneous action of both an axial tensile load and a transverse local compression may be formulated in the following form:

Fracture will take place when the combination of values of the axial tensile load P and the transverse local compression Q reaches the failure locus expressed by a linear relationship of the type $P + k\,Q = P_0$, where P_0 is the maximum load in pure tension.

To determine the fracture locus, standard tension tests (in the absence of any lateral compressions) are required to obtain the maximum load in tension P_0 (ultimate tensile strength of the material), and fracture tests under simultaneous tensile loading and lateral compression to obtain the dimensionless constant k.

Table 2 Mechanical properties of the steel used in the notched specimens (initial diameter of the wire before machining the notches: 12 mm)

Young's Modulus E (Gpa)	Yield Strength σ_Y (MPa)	U.T.S. σ_R (MPa)	Elongation UTS (%)	Ramberg-Osgood $\varepsilon = \sigma/E + (\sigma/P)^n$	
				P(MPa)	n
199	600	1151	6.1	2100	4.9

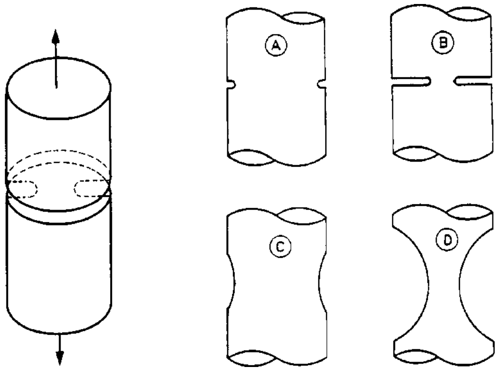

Fig. 4 Axisymmetric notched specimens subjected to tension loading

3. Notched wires under tension loading

Defects such as notches (i.e., with root radius different from zero) are very frequent in structural components as a consequence of very different kinds of damage (Elices 1985). In addition, notched specimens generate a triaxial stress distribution near the notch, which allows a detailed analysis of the influence of stress state and triaxiality on ductile failure (Hancock and Mackenzie 1976, Mackenzie *et al*. 1977, Hancock and Brown 1983) and microscopic mechanisms of fracture (Boonchukosol and Gasc 1979, Beremin 1980).

In a previous paper (Toribio 1997) a fracture criterion was proposed for high-strength steel subjected to multiaxial stress states produced by notches of very different geometries. The research included a fractographic study of the microscopic modes of fracture by scanning electron microscopy, and a numerical analysis by the finite element method to compute the distribution of continuum mechanics variables in the samples at the fracture instant.

The material was a high-strength pearlitic steel whose mechanical properties appear in Table 2. Fracture tests under tension loading were performed on axisymmetric notched specimens with a circumferentially-shaped notch (Fig. 4). Four notch geometries were used, in order to achieve very different stress states in the vicinity of the notch tip and thus very distinct *constraint* situations, thus allowing an analysis of the influence of such factors on the micromechanical fracture processes.

The dimensions of the specimens named A, B, C and D throughout this paper were the following:

- Geometry A : $R/D = 0.03$, $A/D = 0.10$
- Geometry B : $R/D = 0.05$, $A/D = 0.39$
- Geometry C : $R/D = 0.36$, $A/D = 0.10$

• Geometry D : R/D = 0.40, A/D = 0.39

where R is the notch radius, A the notch depth and D the external diameter of the specimen (D=11.25 mm after machining).

Geometries A, B and C exhibited a macroscopically brittle fracture behaviour; geometry D was the only one that exhibited a macroscopically ductile behaviour, with a clear decrease in load. Fracture was assumed to occur at the maximum load point for all geometries, which represents the failure situation or condition of engineering instability under load control (Toribio 1997).

Fractographic analysis of all fractured specimens was carried out by means of scanning electron microscopy. Three conventional microscopic fracture modes were observed: *micro-void coalescence* (MVC, zone in which the fracture process initiates), *cleavage-like* (zone corresponding to brittle fracture in an unstable manner), and *shear lip* (zone of final fracture when it is clearly ductile).

Geometry A presented a fracture surface macroscopically plane, with a microscopic appearance of oriented cleavage. Geometry B showed a fracture surface macroscopically plane, with a microscopic feature created by cleavage without a preferential orientation, i.e., with river patterns randomly oriented on the fracture surface. The fracture surface of geometry C was plane from the macroscopic point of view, the microscopic feature being of cleavage-like type, with a predominant orientation starting from the initiation point, similar to geometry A. Geometry D showed a typical *cup and cone* fracture surface (macroscopic point of view). Microscopically, fracture initiated by MVC at the center of the sample, and propagated in a stable manner, also by MVC, covering almost the whole cross-sectional area.

After performing an elastic-plastic finite-element analysis of the stress-strain state at the fracture instant, different macroscopic (continuum mechanics) variables were checked to formulate the fracture criterion for high-strength steel notched bars. Two candidate variables were considered for the formulation of the fracture criterion, and their distribution at the fracture instant analyzed:

(1) The *strain energy density*, defined as:

$$\omega = \int_0^{\varepsilon} \sigma \bullet d\varepsilon \tag{6}$$

where σ and ε are respectively the stress and strain tensors and • is the inner product of the two

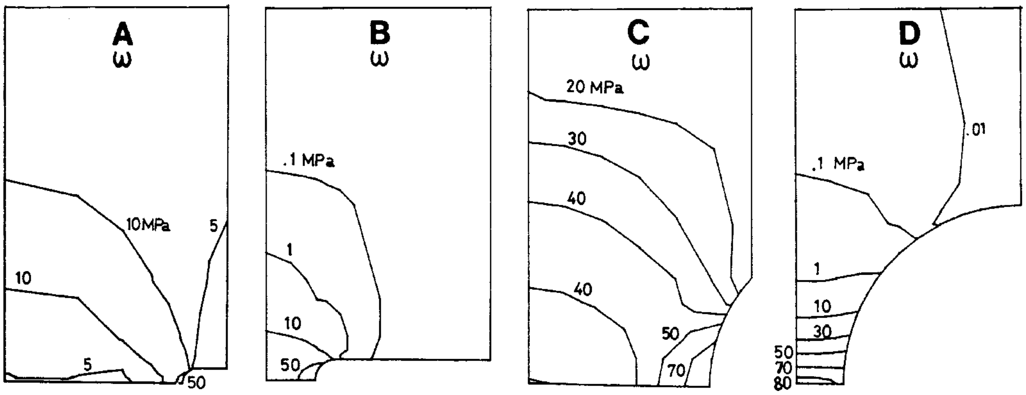

Fig. 5 Distribution of ω in the notched samples at the fracture instant

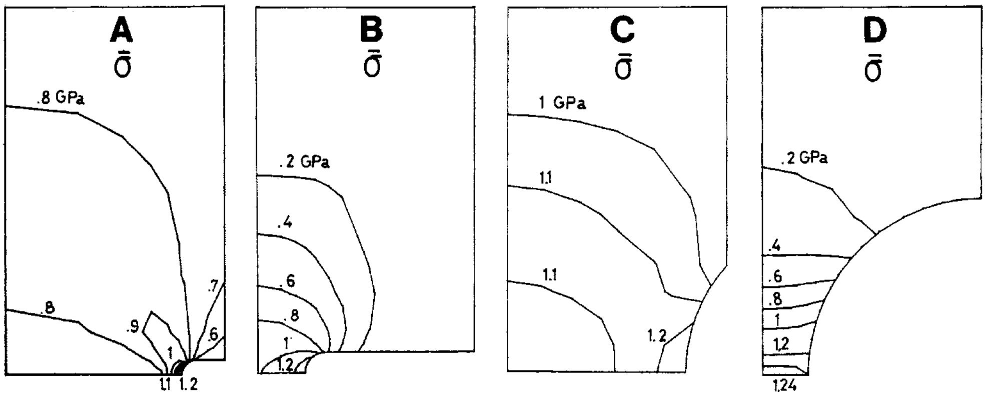

Fig. 6 Distribution of $\bar{\sigma}$ in the notched samples at the fracture instant

tensors. It has been used by Guillemot (1976) and Sih (1985) as the critical variable for fracture processes (*strain energy density criterion*).

(2) The *effective or equivalent stress* in the Von Mises sense, whose expression is:

$$\bar{\sigma} = (3\sigma' \bullet \sigma'/2)^{1/2} \tag{7}$$

where σ' is the stress deviatoric tensor. This variable is a direct function of the distortional part of the strain energy density, i.e., the component associated with shape changes in the material.

Figs. 5 and 6 show respectively the distribution of strain energy density and equivalent stress at the fracture instant, calculated by the elastic-plastic finite element analysis. The plastic zone (line of equivalent stress equal to the yield strength of the material, i.e., 0.6 GPa) clearly exceeds the fracture zone, and seems to have no influence on the fracture process which develops by cleavage. In the matter of the fracture criterion, both the strain energy density and the equivalent stress could be the governing variables, so a more detailed analysis is required to elucidate which is the relevant one. The two distributions are consistent with the fractographic analysis, since the fracture is peripheral (maximum at the notch tip) in geometries A, B and C, and central (maximum at the center of the section) in geometry D.

To establish the criterion, it is necessary to know the average values of the governing variables over the fracture zone or critical region located at the notch tip. The depth of the critical region (x_c) will be several times but never less than the size of the cleavage facet ($x_{CL} \approx 75\,\mu$m in the steel under consideration), related to the prior austenite grain size (Park and Bernstein 1979) and the basic unit of brittle fracture in pearlitic steels (Lewandowski and Thompson 1986). Given the small size of the critical area, one simple method to compute the average with a relative error less than 1%, consists of substituting the average value by the value at the median point.

To compute this average value, the distributions $\omega\,(r, z)$ and $\bar{\sigma}\,(r, z)$ in the fracture zone are required (r and z being the cylindrical coordinates). To this end, a first order polynomial interpolation ($C_1\, r\, z + C_2\, r + C_3\, z + C_4$) was performed in the critical finite element (that located just at the notch tip) on the basis of the numerical results at the Gauss's points at the fracture instant.

Tables 3 and 4 show the average values at the fracture instant of the strain energy density and the

Table 3 Critical values of the strain energy density ω (in MPa)

Geometry	$x_c = x_{CL}$	$x_c = 2\ x_{CL}$	$x_c = 3\ x_{CL}$
A	104.9	84.0	63.2
B	115.3	103.5	91.7
C	96.6	94.9	93.2
D	82.8	82.8	82.9
Average	100±7	91±5	83±7
Variation	28%	20%	32%

Table 4 Critical values of the equivalent stress $\overline{\sigma}$ (in MPa)

Geometry	$x_c = x_{CL}$	$x_c = 2\ x_{CL}$	$x_c = 3\ x_{CL}$
A	1299	1243	1188
B	1324	1299	1274
C	1287	1283	1278
D	1251	1251	1251
Average	1290±15	1270±10	1250±20
Variation	6%	4%	7%

effective or equivalent stress. Averages are calculated over critical sizes (x_c) equal to one, two and three times the size of the cleavage facet (x_{CL}). The equivalent stress is seen to be the relevant variable to establish the criterion, since it remains constant for the different sample geometries, i.e., under different triaxial stress states. The variations of strain energy density are too high for it to be considered a parameter describing fracture under different stress states.

The optimum distance for the fracture criterion to be applied was two cleavage facets (minimal variations of the critical equivalent stress), although the results were not substantially different using one and three cleavage facets. Thus the depth of the critical region (critical size x_c) was assumed to be twice the size of the cleavage facet (or cleavage fracture unit x_{CL}).

Therefore, a simple general criterion can thus be stated on the basis of the distortional part of the strain energy density. This criterion is formulated as follows:

Fracture will take place when the effective or equivalent stress in the Von Mises sense (or, accordingly, the distortional part of the strain energy density) reaches a critical value over a critical region characteristic of the microstructure of the material. This simple criterion may be very useful for engineering design against catastrophic failure in the framework of damage tolerance analyses.

In mathematical form:

$$\langle \overline{\sigma} \rangle = \overline{\sigma}_c \ \text{ over } \ x_c \tag{8}$$

where $<\overline{\sigma}>$ is the average equivalent stress at the fracture instant, $\overline{\sigma}_c$ the critical equivalent stress of the material and x_c the depth of the critical region, the two latter being characteristic parameters of the material, one related to the material toughness and the other to microstructural features. This fracture criterion has been successfully applied to the modelling of the fracture process in hydrogen

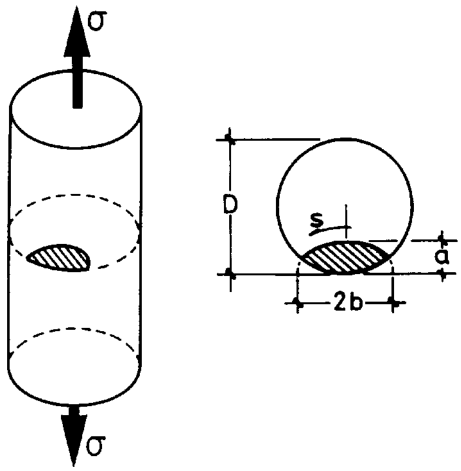

Fig. 7 Geometry of the cracked bar

environment of notched samples of the same high-strength steel as used in this work (Toribio and Elices 1992).

For the pearlitic steel used in this research, the characteristics of strength and microstructure (parameters of the material) are:

$$\overline{\sigma}_c = 1270 \pm 10 \text{ MPa} \tag{9}$$

$$x_c = 2\, x_{CL} = 150 \ \mu\text{m} \tag{10}$$

In a particular situation, these characteristics of strength ($\overline{\sigma}_c$) and microstructure (x_c) are parameters of the material which can be obtained by performing fracture tests on notched bars and posterior numerical analysis to compute the distribution of continuum mechanics variables at the fracture instant.

4. Cracked wires under tension loading

The topic of the fracture criterion for high-strength steel cracked bars has received attention in the past in the framework of fracture mechanics analyses (Valiente 1980, Athanassiadis *et al*. 1981, Astiz *et al*. 1986), considering a cylinder with a semielliptical surface crack (Fig. 7). However, the question is far from being fully understood, specially when the fracture process is not purely brittle.

A pre-requisite is the knowledge of the stress intensity factor K_I for the considered geometry and loading mode: a cylinder subjected to tension with a part-through crack (assumed to be semi-elliptical) perpendicular to the tensile loading direction, i.e., loaded in mode *I*, as shown in Fig. 7. The stress intensity factor is a function of the crack depth, the aspect ratio and the position on the crack border, i.e.,:

$$K_I = K_I\,(a/D,\ a/b,\ s) \tag{11}$$

where a is the crack depth (minor axis of the ellipse), b the major axis of the ellipse, D the diameter of the bar and s the curvilinear coordinate marking the position of the specific point at the crack front.

A dimensionless stress intensity factor Y may also be defined as:

$$Y = K_I/\sigma\sqrt{\pi a} \tag{12}$$

σ being the remote axial stress on the cross section of the bar (uniform distribution of stress):

$$\sigma = 4F/\pi D^2 \tag{13}$$

where F is the tensile load applied on the cylinder.

With regard to a fracture criterion based on the stress intensity factor ($K_I = K_{IC}$), two formulations may be used, one of them global (energy-based) and the other one local (stress-based). These two approaches have been proposed previously, but no definitive conclusion has been drawn on the better one for describing the fracture process in cracked cylindrical bars.

Firstly, a global fracture criterion (Valiente 1980, Athanassiadis *et al*. 1981, Elices 1985) may be formulated on the basis of energetic considerations, using the strain energy release rate concept. According to this criterion, fracture will take place when the energy release rate reaches a critical value. For a given geometry, it only requires a single-parameter approach. Thus an average value of the energy release rate G^* along the crack front may be computed as follows:

$$G^* = \frac{1}{2s}\int_{-s}^{+s}\frac{K_I^2}{E'}ds \tag{14}$$

where E' is the generalized Young's modulus, i.e., $E' = E$ in plane stress (bar surface) and $E' = E/(1-\nu^2)$ in plane strain (crack center). Another possibility is to evaluate the specimen compliance and calculate the energy release rate and thus the stress intensity factor from it. This method was used by Valiente (1980), leading to the following expression:

$$K_I^* = Y^*(a/D)\ \sigma\sqrt{\pi a} \tag{15}$$

where σ is the remote axial stress, a the crack depth and $Y^*(a/D)$ a dimensionless function obtained by a polynomial fitting after a finite element analysis. Such a function is given by:

$$Y^*(a/D) = [0.473 - 3.286(a/D) + 14.797(a/D)^2]^{1/2}[(a/D)-(a/D)^2]^{-1/4} \tag{16}$$

From the results presented by Valiente (1980) using precracked rods of different materials, it may be concluded that global criteria seem to be more adequate for fracture situations with a certain degree of plasticity, i.e., when not purely brittle materials are involved and the microscopic fracture process develops by micro-void coalescence.

Secondly, a local fracture criterion (Astiz *et al*. 1986) may be considered. This criterion was rigourously formulated by Bui and Dang Van (1979) in the form:

$$\mathrm{Sup}_\Gamma\, K_I(s) = K_{IC} \tag{17}$$

where Sup is the operator displaying the maximum value of a given variable (K_I in this case) in a given domain Γ (in this case the domain Γ is the crack line). To apply this local fracture criterion, a biparametric K-solution (depending not only on the crack depth but also on the crack aspect ratio) is required at any point of the crack. It was obtained by Astiz (1986) using the finite element method with singular elements and a virtual crack extension technique to compute the stress intensity factor

Table 5 Values of coefficients C_{ij} to compute the stress intensity factor in cracked cylinders

C_{ij}	$j = 0$	$j = 1$	$j = 2$	$j = 3$
$i = 0$	1.118	–0.171	–0.339	0.130
$i = 2$	1.405	5.902	–9.057	3.032
$i = 3$	3.891	–20.370	23.217	–7.555
$i = 4$	8.328	21.895	–36.992	12.676

Table 6 Nomenclature, diameter reduction and mechanical properties of the steels used in the cracked specimens

Steel	A0	A1	A2	A3	A4	A5	A6
D_i (mm)	12.00	10.80	9.75	8.90	8.15	7.50	7.00
D_i/D_0	1	0.90	0.81	0.74	0.68	0.62	0.58
E (GPa)	197.4	201.4	203.5	197.3	196.7	202.4	198.8
σ_Y (GPa)	0.686	1.100	1.157	1.212	1.239	1.271	1.506
σ_R (GPa)	1.175	1.294	1.347	1.509	1.521	1.526	1.762
P (GPa)	1.98	2.26	2.33	2.49	2.50	2.74	2.34
n	5.89	8.61	8.70	8.45	8.69	7.98	11.49

E: Young's modulus, σ_Y: yield strength, σ_R: ultimate tensile stress (U.T.S.)
P, n: Ramberg-Osgood parameters: $\varepsilon = \sigma/E+(\sigma/P)^n$

at any point of the crack front, and particularly at the crack center (i.e., at s=0 where the maximum value is achieved for a/b<1):

$$K_I{**} = Y{**}\,(a/D,\ a/b)\ \sigma \sqrt{\pi a} \tag{18}$$

In this case the dimensionless stress intensity factor is:

$$Y{**}\,(a/D,\ a/b) = \sum_{\substack{i=0\\ i\neq 1}}^{4} \sum_{j=0}^{3} C_{ij}\,(a/D)^i\,(a/b)^j \tag{19}$$

and the coefficients C_{ij} are given in Table 5 (Astiz 1986). This local fracture criterion has been successfully applied to the fracture of cracked cylindrical bars of reinforcing steel displaying linear-

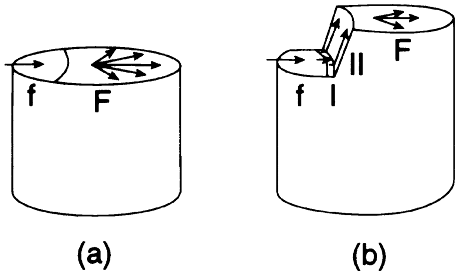

Fig. 8 Fracture modes in slightly drawn (a) and heavily drawn (b) steels

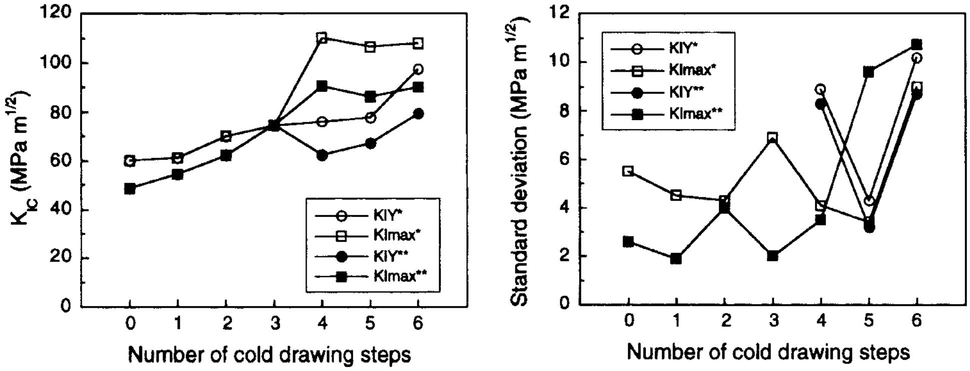

Fig. 9 Critical values of the stress intensity factor and standard deviations

elastic behaviour and brittle fracture at low temperature (Astiz *et al.* 1986).

To check the most adequate fracture criterion at different failure conditions, high strength pearlitic steels with different degrees of cold drawing were used, associated with intermediate steps of the manufacturing process from the hot rolled bar to the prestressing steel wire. Table 6 gives the nomenclature, diameter reduction and mechanical properties of all the steels. After fatigue precracking, the cracked rods were subjected to monotonic tensile loading up to fracture, so as to evaluate the fracture load and the critical crack dimensions.

As shown in Fig. 8, while the fracture behaviour of slightly drawn steels (A0-A3) was isotropic, the most heavily drawn steels (A4 to A6) exhibited anisotropic fracture behaviour with crack deflection and a step oriented 90° in relation to the initial propagation direction by fatigue in mode I. This 90° step is thus parallel to the wire axis or cold drawing direction, a consequence of the marked microstructural orientation induced by cold drawing (Toribio and Ovejero 1998a, Toribio and Ovejero 1998b).

The fractographic analysis of the broken specimens (Toribio and Toledano 2000) revealed that the micromechanisms of fracture also depend on the cold drawing level, from predominant cleavage (brittle) in slightly drawn steels to predominant micro-void coalescence (ductile) in heavily drawn steels (in addition to the 90° step which appears in these steels). This evolution from brittle to ductile microscopic mode of fracture takes place progressively as the degree of cold drawing increases.

In a previous paper (Toribio and Toledano 1999) the application of both the global and the local fracture criteria was discussed in relation to the appearance of the load-displacement plots during the fracture tests and the fractographic analysis. The results are summarized in Fig. 9 which shows the critical values of the stress intensity factor as a function of the number of cold drawing steps undergone by the steels, as well as the experimental standard deviations.

Four characteristic stress intensity values candidates to fracture toughness may be evaluated from the test results: (i) K_{IY}* at fracture initiation using a global fracture criterion; (ii) K_{IY}** at fracture initiation using a local fracture criterion; (iii) $K_{I\,\mathrm{max}}$* at final fracture using a global fracture criterion; (iv) $K_{I\,\mathrm{max}}$** at final fracture using a local fracture criterion. Distinction between fracture initiation and final fracture is only required in heavily drawn steels (A4 to A6).

A local fracture criterion seems to be the most adequate for brittle failure (taking place in slightly drawn steels). This is consistent with a micromechanism of fracture of the *weakest link* type, according to which fracture occurs when a single point reaches the critical condition of fracture. Thus, for slightly drawn steels breaking in purely brittle mode:

$$K_{IC} = K_{IY}^{**} = K_{I\,\max}^{**} \tag{20}$$

Conversely, a global fracture criterion appears to be most suitable for ductile failure, or brittle failure after a previous ductile development taking place in heavily drawn steels, which is consistent with a micromechanism of fracture of the *process zone* type (fracture occurs when the critical condition is reached over a certain area). Thus, for heavily drawn steels breaking in a more ductile mode:

$$K_{IC}^{(i)} = K_{IY}^{*} \tag{21}$$

$$K_{IC}^{(f)} = K_{I\,\max}^{*} \tag{22}$$

Apart from its adequacy for more ductile fracture processes, the global fracture criterion accounts for the anisotropic fracture behaviour caused by the markedly oriented microstructure (in a direction parallel to the wire axis) of heavily drawn steels as a consequence of the drawing process. Therefore, this global criterion could be useful for fracture processes in high-strength steel cracked wires with certain degree of ductility and anisotropy, which is fully consistent with the results obtained by Valiente (1980).

In spite of the fact that a global criterion describes better the fracture process in heavily drawn steels, the use of a local one could be considered as a conservative approach to damage tolerance design. Thus, for the sake of uniqueness, a common fracture criterion valid for any degree of cold drawing in high-strength prestressing steel wires could be formulated in the following form:

Fracture will take place when the maximum stress intensity factor at any point of the crack front reaches a critical value which can be considered as a material property: the fracture toughness of the considered material.

Its mathematical form is given in Eq. (17). The fracture toughness K_{IC} (a material property) can be obtained by performing fracture tests on cracked bars and posterior computation of the critical value of the maximum stress intensity factor along the crack border by using the expressions (18) and (19).

5. Conclusions

Failure criteria were proposed as design criteria for structural engineering, covering different practical situations with different degrees of stress triaxiality in the structural element under consideration: the smooth wire under transverse load, and both the notched bar and the cracked wire under tension loading, which represent many practical situations.

It was seen that the engineering fracture criteria (macroscopic) are based on the microscopic mechanisms of failure ranging from microvoid coalescence (typically ductile) to cleavage-like (typically brittle), which shows the links between structural engineering (on one side) and fracture mechanics and materials science (on the other side).

Material resistance to failure is represented by the critical parameter at the fracture situation which may be experimentally evaluated by means of fracture tests to determine the failure locus (smooth wire under transverse load), the critical equivalent stress (notched wire in tension) or the fracture toughness (cracked wire in tension).

Acknowledgements

The financial support of this work by the Spanish CICYT (Grant MAT97-0442) and *Xunta de Galicia* (Grants XUGA 11801B95 and XUGA 11802B97) is gratefully acknowledged. In addition, the authors wish to express their gratitude to EMESA TREFILERIA S.A. [Grupo ACERALIA] (La Coruña, Spain) and TREFILERIAS QUIJANO (Los Corrales de Buelna, Cantabria, Spain) for providing the steels used in the experimental programme.

References

Astiz, M.A. (1986), "An incompatible singular elastic element for two- and three- dimensional crack problems", *Int. J. Fracture*, **31**, 105-124.

Astiz, M.A., Elices, M. and Valiente, A. (1986), "Numerical and experimental analysis of cracked cylindrical bars", in *Fracture Control of Engineering Structures/ECF 6* (Edited by H.C. van Elst and A. Bakker). EMAS, West Midlands, U.K., 65-74.

Athanassiadis, A., Boissenot, J.M., Brevet, P., Francois, D. and Raharinaivo, A. (1981), "Linear elastic fracture mechanics computations of cracked cylindrical tensioned bodies", *Int. J. Fracture*, **17**, 553-566.

Beremin, F.M. (1980), "Influence de la triaxialit des contraintes sur la rupture par dhirement ductile et la rupture fragile par clivage d'un acier doux", *Journal de Méoanique Appliqu*, **4**(3), 327-342.

Boonchukosol, K. and Gasc, C. (1979), "Influence de l'éat de contrainte sur les conditions de rupture des aciers", *Journal de Méoanique Appliqu*, **3**(1), 105-118.

Bui H.D. and Dang Van K. (1979), "Généralisation de la thérie de la rupture de Griffith", *J. Manique Appliqu* **3**(2), 205-225.

CEN (1992), *Eurocode 3-1992 ENV 1993-1-1 Design of Steel Structures Part 1.1: General Rules and Rules for Buildings*, European Commitee for Standardization, Brussels.

Elices, M. (1985), "Fracture of steels for reinforcing and prestressing concrete", in *Fracture Mechanics of Concrete: Structural Application and Numerical Calculation* (Edited by G.C. Sih and A. DiTommaso). Martinus Nijhoff Publishers, Dordrecht, The Netherlands, 226-271.

Guillemot, L.F. (1976), "Criterion for crack initiation and spreading", *Engng. Fracture Mech.*, **8**, 239-253.

Hancock, J.W. and Brown, D.K. (1983), "On the role of strain and stress state in ductile failure", *J. Mech. Phys. Solids*, **31**, 1-24.

Hancock, J.W. and Mackenzie, A.C. (1976), "On the mechanisms of ductile failure in high-strength steels subjected to multi-axial stress-states", *J. Mech. Phys. Solids*, **24**, 147-169.

Johnson, W. and Mellor, P.B. (1986), *Engineering Plasticity*, Ellis Horwood Limited, Chichester.

Lewandowski, J.J. and Thompson, A.W. (1986), "Effects of the prior austenite grain size on the ductility of fully pearlitic eutectoid steel", *Metall. Trans.*, **17A**, 461-472.

Mackenzie, A.C., Hancock, J.W. and Brown, D.K. (1977), "On the influence of state of stress on ductile failure initiation in high strength steels", *Engng. Fracture Mech.*, **9**, 167-188.

Park, Y.J. and Bernstein, I.M. (1979), "The process of crack initiation and effective grain size for cleavage fracture in pearlitic eutectoid steel", *Metall. Trans.*, **10A**, 1653-1664.

Sih, G.C. (1985), "Mechanics and physics of energy density theory", *Theor. Appl. Fracture Mech.*, **4**, 157-173.

Toribio, J. (1997), "A fracture criterion for high-strength steel notched bars", *Engng. Fracture Mech.*, **57**, 391-404.

Toribio, J. and Elices, M. (1992), "The role of local strain rate in the hydrogen embrittlement of round-notched samples", *Corros. Sci.*, **33**, 1387-1409.

Toribio, J. and Ovejero, E. (1998a), "Microstructure orientation in a pearlitic steel subjected to progressive plastic deformation", *J. Mater. Sci. Lett.*, **17**, 1037-1040.

Toribio, J. and Ovejero, E. (1998b), "Effect of cold drawing on microstructure and corrosion performance of high-strength steel", *Mech. Time-Dependent Mater.*, **1**, 307-319.

Toribio, J. and Toledano, M. (1999), "A fracture criterion for prestressing steel cracked wires", in *Advances in*

Steel Structures/ICASS'99 (Edited by S.L. Chan and J. G. Teng). Elsevier Science, Oxford, U.K., 947-954.

Toribio, J. and Toledano, M. (2000), “Fatigue and fracture performance of cold drawn wires for prestressed concrete”, *Constr. Building Mater.*, **14**, 47-53.

Valiente, A. (1980), “Criterios de fractura para alambres”, Ph. D. Thesis, Polytechnic University of Madrid.

Valiente, A., Elices, M. and Toribio, J. (1988), “Tensile strength of prestressing steels under transversal loads”, in *Failure Analysis. Theory and Practice/ECF7* (Edited by E. Czoboly). EMAS, West Midlands, U.K., 555-557.

CC